Molecular Vision 2022; 28:83-95 <http://www.molvis.org/molvis/v28/83>
Received 22 March 2021 | Accepted 18 May 2022 | Published 20 May 2022

Comprehensive circular RNA expression profiling with associated ceRNA network in orbital venous malformation

Jie Yu, Peiwei Chai, Yixiong Zhou, Renbing Jia, Yefei Wang

Department of Ophthalmology, Shanghai Key Laboratory of Orbital Diseases and Ocular Oncology, Ninth People's Hospital, Shanghai JiaoTong University School of Medicine, Shanghai, P.R. China

Purpose: Orbital venous malformation (OVM), the most common type of vascular malformation in adults, has a great impact on both visual and cosmetic factors. Circular RNAs (circRNAs) play important roles in various ophthalmological diseases; however, little is known about their function in the pathogenesis of OVM.
Methods: We obtained differentially expressed circRNAs, mRNAs, and miRNAs based on RNA sequencing of four OVM tissues and four normal orbital vascular tissues. The circRNA–mRNA coexpression network and circRNA–miRNA–mRNA and competing endogenous RNA (ceRNA) networks were constructed using miRanda software. Gene Ontology (GO) and Kyoto Encyclopedia of Genes and Genomes (KEGG) pathway analyses were performed to identify the up- and downregulated mRNAs in the circRNA–miRNA–mRNA ceRNA network.
Results: Overall, we identified 45 upregulated and 144 downregulated circRNAs, as well as 2,175 upregulated and 1,274 downregulated mRNAs and 156 upregulated and 168 downregulated miRNAs in OVM samples compared with normal orbital vascular tissues. The expression changes of mRNAs and circRNAs detected by quantitative real-time PCR (qRT-PCR) were in line with the RNA-seq results. Then, a ceRNA regulatory network was constructed with these differentially expressed circRNAs, mRNAs, and miRNAs. GO functional analysis revealed that most related biological processes involved extracellular matrix organization, positive regulation of actin nucleation, and so on, which were thought to be involved in the evolution of OVM. KEGG pathway analysis of upregulated mRNAs showed that mucin-type O-glycan biosynthesis, glycosaminoglycan degradation, and the *PI3K* (Gene ID: 5290; OMIM: 613089)-*AKT* (Gene ID: 207; OMIM: 114500) signaling pathway were all enriched in OVM samples.
Conclusions: Our study provides novel insight into the regulatory mechanism of circRNAs, miRNAs, and mRNAs in the pathogenesis of OVM.

(First two authors contributed equally to this report.)

Orbital venous malformation (OVM) is one of the most common types of vascular malformations, with an incidence of approximately 0.94 per 10 million people [1], affecting more middle-aged women than men [2]. It is a congenital vascular disease caused by aberrant angiogenesis during embryonic development. The lesions enlarge slowly, and common clinical presentations include proptosis, diplopia, exophthalmos, optic nerve compression, and relative visual field alterations [3-5]. Despite an improved understanding of the pathophysiology and hemodynamics of OVM and advances in new treatment techniques, such as sclerotherapy, laser therapy, embolization, and radiotherapy, the management of OVM remains challenging, with multiple complications and a high recurrence rate [6]. This is due to the deep or internal location close to visually critical elements, the risks of bleeding during the operation, and the invasive nature of OVM [6-8].

In recent years, an increasing number of researchers have attempted to elucidate the pathogenic mechanism of OVM. Transcriptional profiling analysis of OVM samples has revealed that vascular endothelial growth factor (VEGF) and autophagy pathways were upregulated and Hippo, Wnt, and hedgehog signaling pathways were downregulated. An angiogenesis antibody array showed that plasma leptin and epidermal growth factor (EGF) levels were elevated significantly in OVM patients [9]. GPAA1 (c.968A > G) was reported as a novel variant causing inherited vascular anomalies. Mutations that resulted in scarce expression of the GPAA1 protein and localization alterations were proven to impair angiogenesis and vascular remodeling both in vitro and in vivo [10]. In addition, the MC4R (Gene ID: 4160; OMIM: 618406) mutation was found to cause aberrant

Correspondence to: Yefei Wang, Ninth People's Hospital, Shanghai JiaoTong University School of Medicine, Shanghai, 200025, P.R. China; email: paper34@163.com

expression levels of some *PI3K*/*AKT*/*mTOR* (Gene ID: 2475; OMIM: 607341) downstream genes and a concentration of cAMP, which contributes to the pathogenesis of OVM [11]. Nevertheless, the pathogenesis of OVM remains unclear.

CircRNAs are novel endogenous noncoding RNAs characterized by a closed continuous ring structure in which the 3′ and 5′ ends are ligated covalently without polarity or poly (A) tails [12]. They mainly function as competing endogenous RNAs (ceRNAs) that specifically bind to miRNAs like sponges and thereby upregulate the expression of miRNA-related target genes [13]. Studies have shown that they play pivotal roles in multiple ophthalmologic diseases. For example, in diabetic retinopathy, circular RNA-ZNF532 induced vascular dysfunction and retinal pericyte degeneration by acting as a miR-29a-3p sponge and increasing the expression of targeted genes, including *NG2*, *CDK2*, and *LOXL2* [14]. In addition, 163 circRNAs with different expression levels were identified in thyroid-associated ophthalmopathy, and the circRNA_14940-CCND1-Wnt signaling pathway may be a vital regulatory pathway in its pathogenesis [15]. These studies highlighted the important functions of circRNAs in ophthalmologic diseases; however, the role of circRNAs in the pathogenesis of OVM remains unclear.

In this study, we identified OVM-related dysregulated circRNAs, as well as differentially expressed mRNAs and microRNAs (miRNAs), in OVM samples compared with normal controls using RNA-seq. Quantitative real-time PCR (qRT-PCR) was then performed to verify the reliability of the RNA-seq data. Moreover, using these aberrantly expressed circRNAs, a circRNA-mRNA coexpression network and a circRNA-associated ceRNA network were constructed to provide novel genetic insights into the pathogenic mechanism of OVM.

METHODS

Patients and samples: Nine samples were taken from OVM patients diagnosed with pathological verification at the Ninth People's Hospital, Shanghai Jiao Tong University School of Medicine, between January 2017 and June 2019 (Appendix 1), as previously reported [9]. Nine normal orbital vascular specimens were collected from patients with orbital trauma or cosmetic surgery (Appendix 2), as previously reported [9]. Specimens were only used with informed consent from the patients, and this study was approved by the research ethics committee of the Ninth People's Hospital, Shanghai Jiao Tong University School of Medicine.

RNA extraction, library preparation, and sequencing: Total RNA was isolated from the OVM samples of four patients and four normal orbital vascular tissues using a mirVana miRNA Isolation Kit (Ambion, Austin, TX) following the manufacturer's instructions. Briefly, the tissue samples were lysed in a denaturing lysis solution, and then the RNA was extracted with Acid-Phenol: Chloroform to remove most of the other cellular components. Further purification was performed on a glass-fiber filter to yield either total RNA or miRNA-enriched fractions. Finally, solutions formulated specifically for miRNA retention was used to avoid the loss of small RNA. Then, cDNA libraries were constructed using a TruSeq Stranded Total RNA Kit with Ribo-Zero Gold (Illumina, San Diego, CA) following the manufacturer's protocol. Quality validation of the libraries was performed using an Agilent 2100 Bioanalyzer (Agilent Technologies), and high-throughput RNA-seq of these libraries was conducted on the Illumina sequencing platform (HiSeqTM 2500).

For miRNA sequencing, a Small RNA Sample Prep Kit (Illumina) was employed to construct libraries following the manufacturer's instructions. The validity of the library quality control was verified by an Agilent 2100 Bioanalyzer (Agilent Technologies, Palo Alto, CA), and sequencing was conducted on a HiSeq X Ten.

Differential expression RNA analysis: We used DESeq software packages [16] to analyze the differentially expressed mRNAs, circRNAs, and miRNAs. The cutoff criterion of differentially expressed RNAs was |log2 FC (fold change) |≥1 and $p<0.05$. Then, hierarchical cluster analysis was conducted using the pheatmap package (Version 1.0.8) [17] with these differentially expressed RNAs.

qRT-PCR: Total RNA was isolated from OVM samples and normal orbital vascular tissues using the mirVana miRNA Isolation Kit (Ambion), following the manufacturer's protocol. Thereafter, the RNA was reverse transcribed into cDNA using the PrimeScript RT reagent kit (Takara Bio, Shiga, Japan). Then, qRT-PCR was performed using SYBR Green PCR master mix (Life Technologies, Carlsbad, CA) and an RT-PCR system (Applied Biosystems, Waltham, MA). The housekeeping gene *ACTB* was the control for PCR product quantification and normalization. The primers for circRNAs and mRNAs are listed in Table 1.

Construction of circRNA-mRNA coexpression network: The coexpression analysis of the circRNA-mRNA network was constructed according to the differential expression levels of mRNAs and circRNAs in OVM and normal control samples. We used the Pearson's correlation coefficient of mRNAs and circRNAs >0.80 and $p<0.05$ to construct the coexpression network and Cytoscape software (Version 3.2.1) to visualize it.

Table 1. Primers used in this study RT-qPCR primers.

Gene	Sequences (5′-3′)
ACTB-Forward	TGGCACCCAGCACAATGAA
ACTB-Reverse	CTAAGTCATAGTCCGCCTAGAAGCA
CALD1-Forward	TCTGTGCAGAAAAGCAGTGGT
CALD1-Reverse	GCAGGAACAGGAAGATCCGA
RHOA-Forward	GGTGGATGGAAAGCAGGTAGA
RHOA-Reverse	GCACGTTGGGACAGAAATGC
AES-Forward	CACAAAGCAGGCATTCGGG
AES-Reverse	ACATTCGAGCTTGAGGCTGT
CTSD-Forward	GATTCAGGGCGAGTACATGAT
CTSD-Reverse	GGACAGCTTGTAGCCTTTGC
LAPTM5-Forward	GGCTCTTTCCCCTTCAGTGTC
LAPTM5-Reverse	AGGTACTTCTCCCGGTTCACAT
circRNA_2189-Forward	ATGGGTTACATGCCCAAGAGGG
circRNA_2189-Reverse	AGCGAATACTGCTGTCACCCTT
circRNA_3645-Forward	ATGTTTCCAGTCTGCTGGCCAAG
circRNA_3645-Reverse	TTTCGTAGGAGTGGGAGTGTTGG
circRNA_3192-Forward	GCGAAGACTATCAGGGAATGA
circRNA_3192-Reverse	GGCATGGGGATCATCATCTTT

Construction of a circRNA-associated ceRNA network: The exploration of potential circRNA-associated ceRNA networks was analyzed according to the obtained differentially expressed mRNAs, circRNAs, and miRNAs. CircRNA–miRNA pairs and miRNA–mRNA pairs were predicted using the miRanda tools. These two pairs sharing the same miRNAs were identified as candidate circRNA–miRNA–mRNA competing interactions. Expression correlations between circRNAs, miRNAs, and mRNAs with a threshold of p value <0.05 and Pearson's correlation coefficient >0.85 or < −0.85 were filtered out. Thereafter, the circRNA-associated ceRNA network was constructed using Cytoscape software (Version 3.2.1).

GO and KEGG analysis: The functions of the differentially expressed mRNAs identified from the circRNA-associated ceRNA network were analyzed using Gene Ontology (GO) and Kyoto Encyclopedia of Genes and Genomes (KEGG) pathway analysis. GO analysis used the biologic process (BP), cellular component (CC), and molecular function (MF) to mark genes. KEGG analysis provided annotation information for gene signal transduction and disease pathways. The GO terms and KEGG pathways with p<0.05 were considered to be enriched with statistical significance.

RESULTS

Representative clinical characteristics of OVM patients: In our study, nine OVM tissue samples and nine normal control samples were included; of these, four OVM tissue samples and four normal control samples were sequenced and the other five OVM tissue and five normal control samples were used to validate the sequencing by qRT-PCR. Representative pictures of the patient's appearance are shown in Figure 1A,B. In magnetic resonance imaging (MRI), hypointensity is apparent in T1-weighted images (T1WIs) and hyperintensity in T2-weighted images (T2Wis; Figure 1C,D). Normal control tissues were collected from orbital trauma or cosmetic surgery, as shown with OVM samples in Figure 1E,F. In addition, hematoxylin and eosin (H&E) staining (Appendix 3) and immunohistochemical staining (Appendix 3) of a vascular endothelial cell marker, CD34, showed that both OVM and control samples were vascular tissue.

Identification and characterization of circRNAs: The expression profile of circRNAs in OVM and normal control tissues was detected by RNA-seq, and 9,375 circRNAs were identified. Among these circRNAs, 5,106 were reported in circBase, and 4,269 identified circRNAs were newly discovered (Figure 2A,B). Sequence length analysis revealed that these circRNAs ranged in length from less than 200 nucleotides (nt) to more than 2,000 nt, and most were 200–500 nt or over 2,000 nt (Figure 2C). The circRNA transcripts were

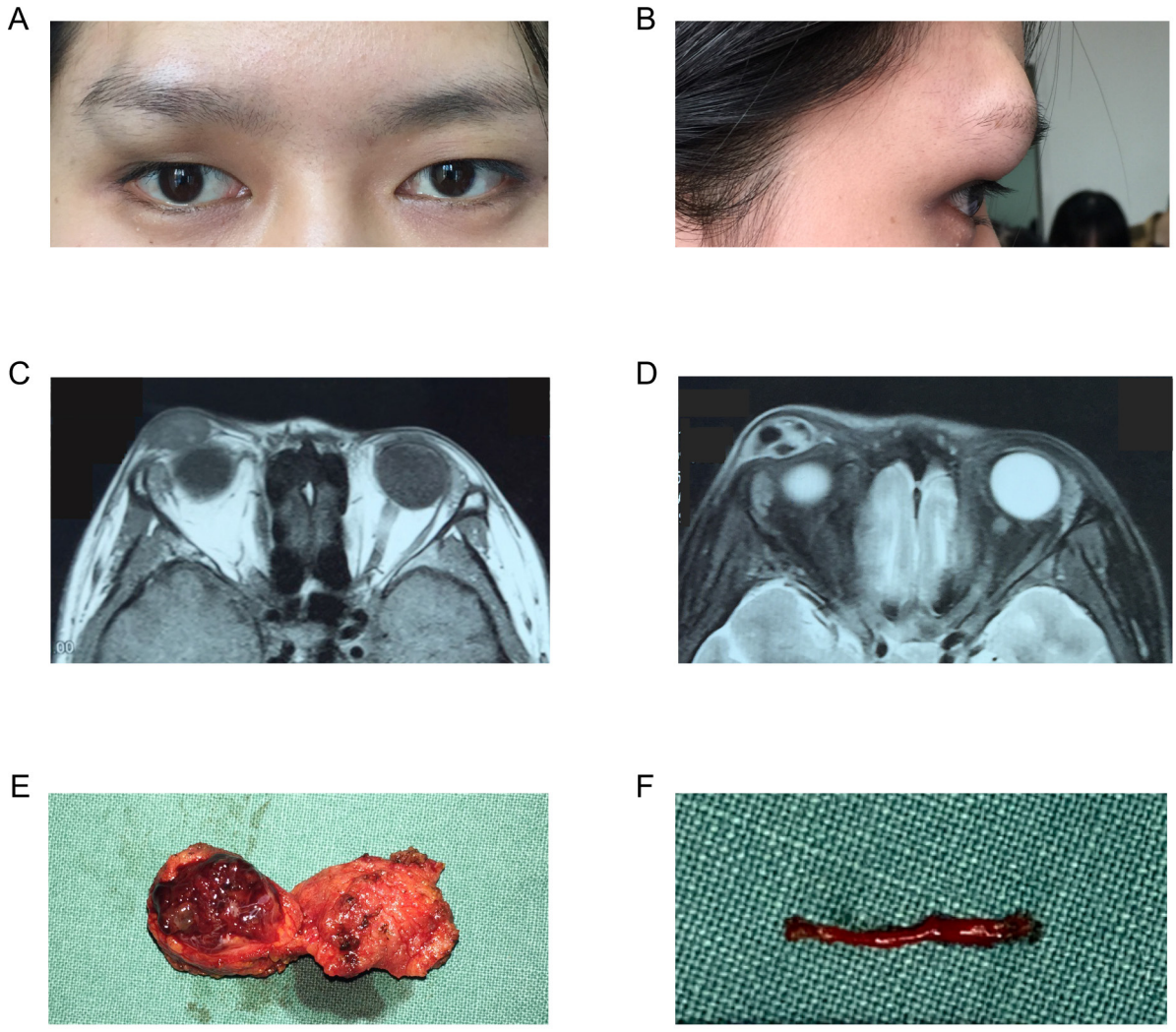

Figure 1. Clinical characteristics of orbital venous malformation (OVM) patients. **A**, **B**: Representative clinical characteristics of patients with OVM. **C**, **D**: Representative Magnetic resonance imaging (MRI) images of patients with OVM, T1-weighted image (T1WI) (**C**), and T2-weighted image (T2WI) (**D**). **E, F**: Images of OVM and normal orbital vascular tissue samples.

broadly distributed throughout the genome, with more on chromosomes 1, 2, and 3 (Figure 2D). In addition, exonic circRNAs accounted for the largest type (Figure 2E), and the number of exons per circRNA mainly ranged from 1 to 6 (Figure 2F). We used reads per million (RPM) values to estimate the expression level of the circRNAs, and there were no significant differences in each sample (Figure 3A,B).

Identification of differentially expressed RNAs: To identify the potential biological role of circRNAs in OVM, we analyzed differentially expressed mRNAs, circRNAs, and miRNAs with thresholds of $|\log2\ FC| \geq 1$ and $p<0.05$. RNA-seq analysis identified 3449 aberrantly expressed mRNAs in OVM, including 2,175 upregulated and 1,274 downregulated mRNAs **(**Figure 4A, Appendix 4). Meanwhile, 45 upregulated and 144 downregulated circRNAs were found in OVM tissues compared with normal controls (Figure 4B, Appendix 5). In addition, 156 miRNAs were upregulated and 168 miRNAs were downregulated in the OVM samples (Figure 4C, Appendix 6). Hierarchical clustering analysis showed that differentially expressed mRNA, circRNA, and miRNA expression patterns among samples were distinguishable (Figure 4D,E).

Validation of differentially expressed mRNAs and circRNAs by qRT-PCR: We performed qRT-PCR to verify the reliability of the differentially expressed circRNAs and mRNAs identified in the OVM tissues and normal controls by RNA-seq.

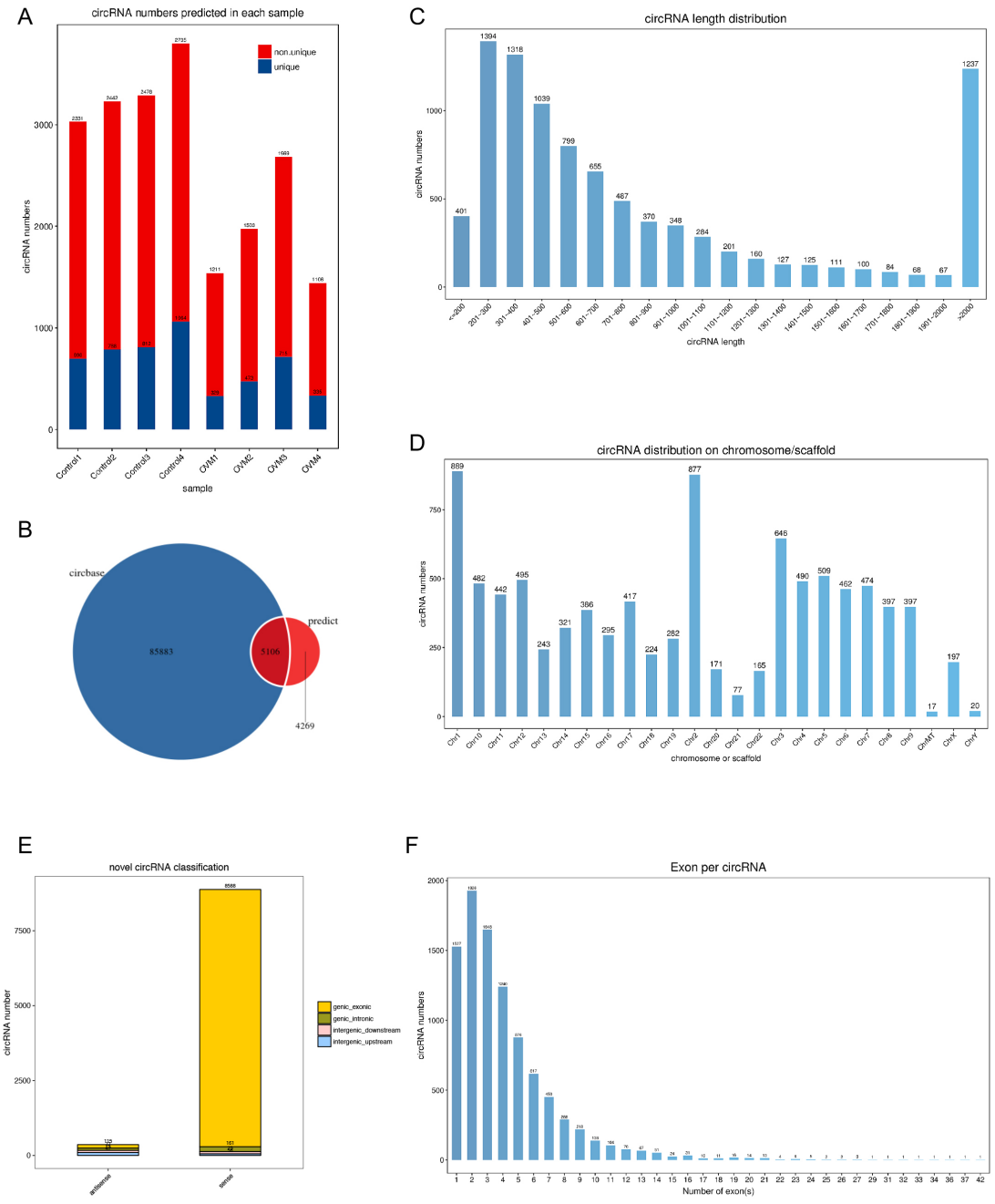

Figure 2. Characterization of identified circular RNAs (circRNAs) in orbital venous malformation (OVM) and normal orbital vascular tissues. **A:** The number of identified circRNAs in OVM (OVM1, OVM2, OVM3, and OVM4) and normal orbital vascular tissues (Control1, Control2, Control3, and Control4). **B**: Venn analysis of identified circRNAs and published circRNAs in circBase. **C**: Length distribution of identified circRNAs. **D**: Chromosome distribution of identified circRNAs. **E**: Classification of identified circRNAs. **F**: The exon number distribution of exon-derived circRNAs.

Five mRNAs (CALD1, RHOA, AES, CTSD, and LAPTM5), and three circRNAs—circRNA_2189 (hsa_circ_0000437 officially), circRNA_3654 (hsa_circ_0000745 officially), and circRNA_3192 (hsa_circ_0003856 officially), were randomly selected. The results revealed that CALD1, RHOA, and AES were downregulated in OVM samples and that CTSD and LAPTM5 were upregulated in OVM samples, which is in accordance with the RNA-seq results (Figure 5A,C). The

qRT-PCR results of circRNA_2189, circRNA_3654, and circRNA_3192 were in line with the RNA-seq data (Figure 5B,D), suggesting that the differentially expressed circRNAs identified via RNA-seq were reliable.

Construction of circRNA-associated ceRNA networks: To investigate the role of circRNAs in OVM, the expression correlations between circRNA and mRNA and ceRNAs (circRNA–miRNA–mRNA) were identified according to the differentially expressed RNAs, including 54 circRNAs, 1,566 mRNAs, 107 miRNAs, and bioinformatic prediction results. We first constructed a coexpression network of the top 100 circRNA–mRNA interactions by Cytoscape

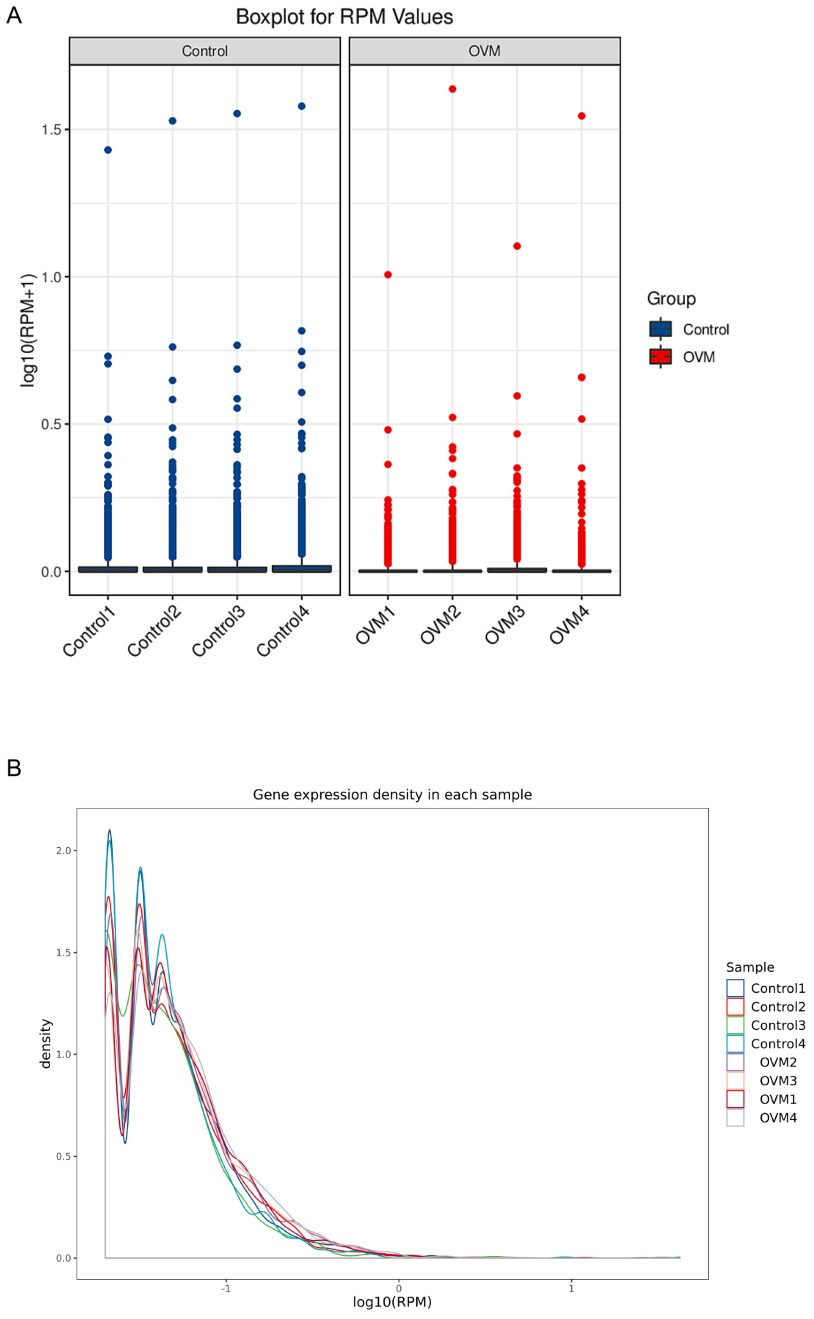

Figure 3. Qualification of circular RNAs (circRNAs) in orbital venous malformation (OVM) and normal orbital vascular tissues. **A**: Box plots of reads per million (RPM) values of circRNAs in OVM and normal orbital vascular tissues. **B**: Density plot of the expression density distribution of circRNAs in OVM and normal orbital vascular tissues.

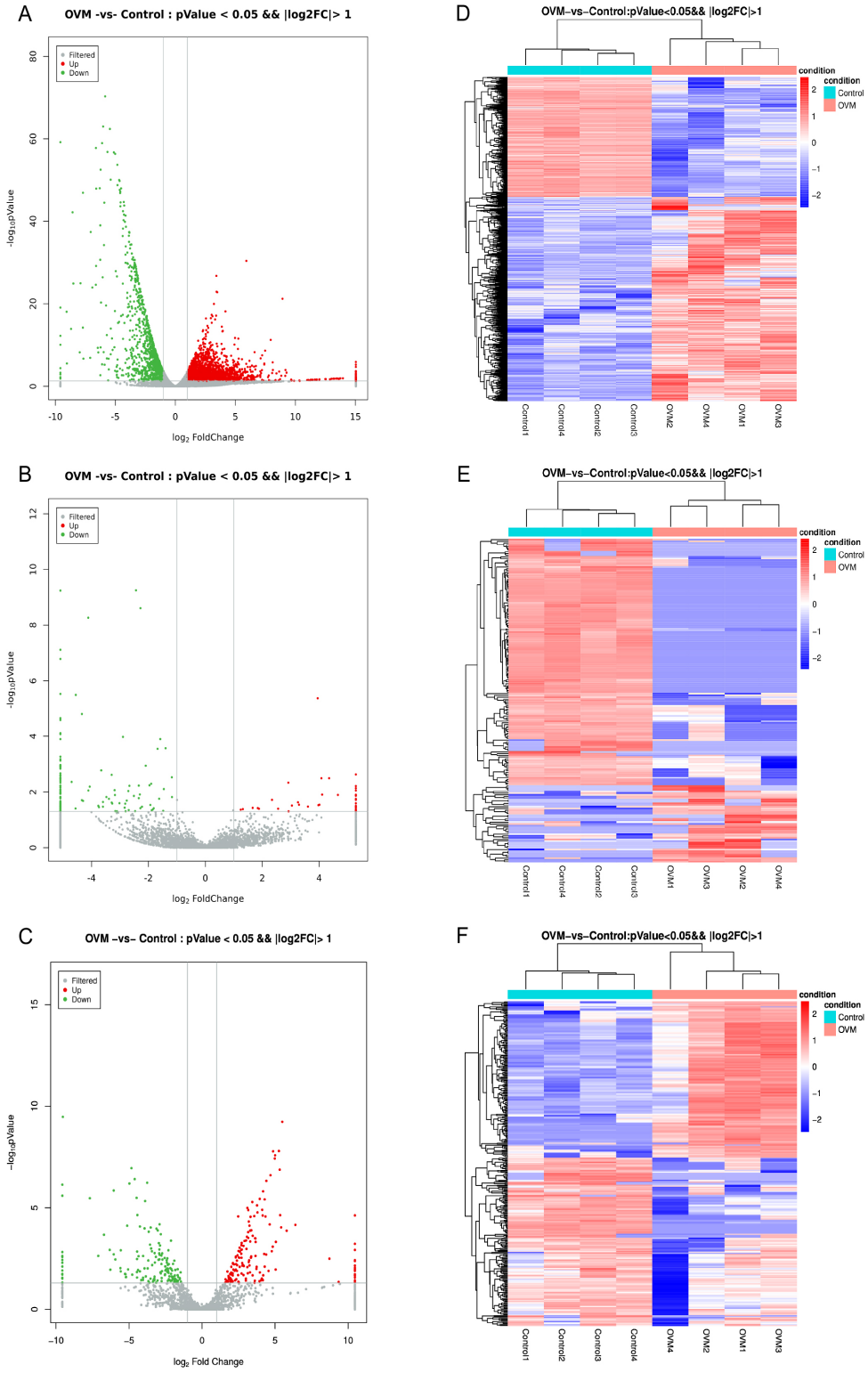

Figure 4. Expression analysis of different RNAs in orbital venous malformation (OVM) and normal orbital vascular tissues. **A**, **B**, **C**: Volcano plot of differentially expressed mRNAs (**A**), circular RNAs (circRNAs) (**B**), and miRNAs (**C**) based on the thresholds of |log2 FC| ≥1 and p<0.05 in OVM and normal orbital vascular tissues. **D**, **E**, **F**: Hierarchical cluster analysis of differentially expressed mRNAs (**D**), circRNAs (**E**), and miRNAs (**F**) in OVM and normal orbital vascular tissues.

3.2.1 (Figure 6). Then, two circRNA-associated ceRNA networks—circRNA_8224 (upregulated in OVM)–miRNAs (downregulated in OVM)–mRNAs (upregulated in OVM) and circRNA_1678 (downregulated in OVM)–miRNAs (upregulated in OVM)–mRNA (downregulated in OVM)—were constructed (Figure 7). These ceRNA network results may provide a new underlying mechanism for OVM.

Functional analyses of dysregulated mRNAs in the ceRNA network: GO and KEGG pathway analyses further explored the potential function of mRNAs involved in the ceRNA network. Based on the GO analysis results, mRNAs with upregulated expression levels were significantly enriched in BPs, such as extracellular matrix organization and positive regulation of actin nucleation; CCs, such as the plasma membrane and adherens junction; and MFs, such as lysophosphatidic acid receptor activity and cell adhesion molecule binding. The downregulated mRNAs were mainly associated with BPs, such as mesenchymal migration and muscle contraction; CCs, such as the Z disc and stress fiber; and MFs, such as actin binding and cadherin binding (Figure 8A-B, Appendix 7 and Appendix 8). According to the results of the KEGG pathway analyses, we identified upregulated mRNAs that participate in pathways, such as mucin-type O-glycan biosynthesis, glycosaminoglycan degradation, and the PI3K-Akt signaling pathway. The downregulated mRNAs were involved in pathways, such as regulation of the actin cytoskeleton, the calcium signaling pathway, and the cAMP signaling pathway (Figure 8C-D, Appendix 9 and Appendix 10). These functional analyses suggested that the circRNA-associated ceRNA network may have multiple regulatory functions in OVM pathogenesis. In addition, we found that most of the genes in the mucin-type O-glycan biosynthesis, glycosaminoglycan degradation and PI3K-Akt signaling pathway were upregulated (Appendix 11), and representative genes in these signaling pathways were verified by qRT-PCR (Figure 8E). We further applied immunohistochemical (IHC) staining to p-PI3K and p-Akt, and the results demonstrated that p-PI3K and p-Akt presented stronger signals in OVM samples (Figure 8F). These data indicate that these pathways may account for OVM.

DISCUSSION

OVM ranks as the most common type of vascular disease in the orbital region, which can cause visual deterioration and cosmetic defects [6]. Recently, great efforts have been made to discover the detailed physiological and pathological mechanisms of OVM, as well as new therapeutic targets and biomarkers of OVM [9,11,18,19]; however, these studies have

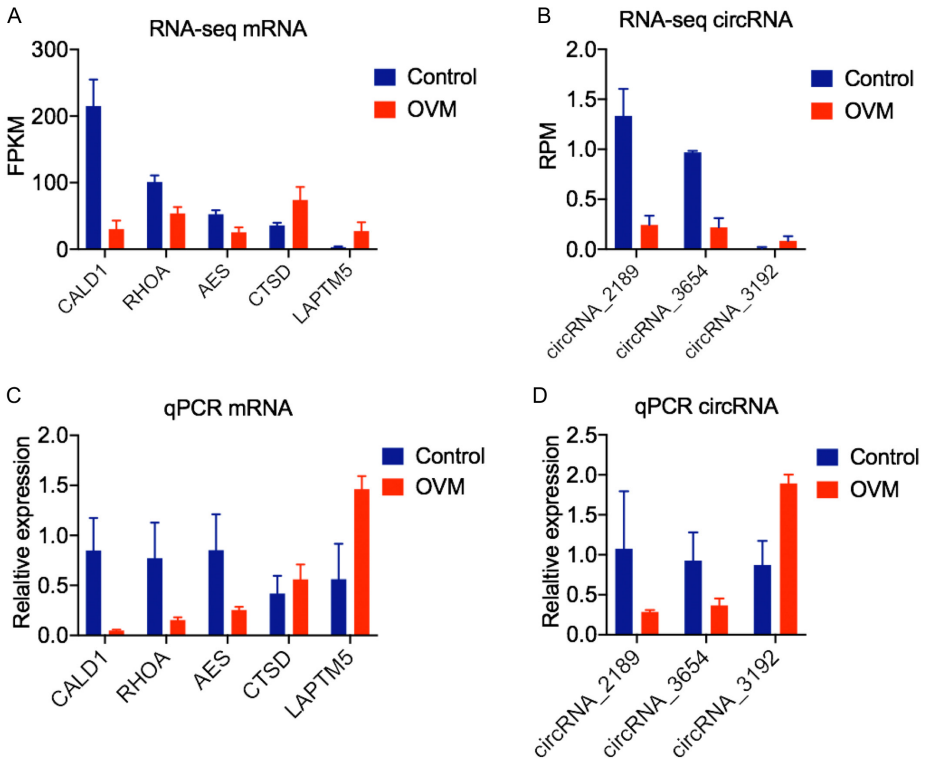

Figure 5. Validation and comparison of mRNA and circular RNA (circRNA) expression levels between quantitative real-time PCR (qRT-PCR) and RNA-seq. **A**, **C**: The expression levels of five mRNAs (CALD1, RHOA, AES, CTSD, and LAPTM5) by RNA sequencing analysis (**A**) and qRT-PCR (**C**). **B**, **D**: The expression levels of three circRNAs (circRNA_2189, circRNA_3654, and circRNA_3192) by RNA sequencing analysis (**B**) and qRT-PCR (**D**).

been limited to protein-coding genes or proteins. CircRNAs are a new kind of functional noncoding RNA that regulates various processes and is involved in numerous diseases [20,21]. However, the circRNA expression profiles and their functions in OVM remain largely unknown. Therefore, in our study, we investigated circRNA, miRNA, and mRNA expression profiles and their potential roles in OVM for the first time.

First, 9,375 circRNAs were identified in total, including 5,106 (54.5%) previously reported circRNAs and 4,269 (45.5%) newly discovered circRNAs. Most of these circRNAs ranged from 200 to 500 nt or were over 2,000 nt in length, which was similar to the results found in many other eye diseases [15,22,23]. In the analysis of chromosome distribution, we found that circRNAs were predominantly located on chromosomes 1, 2, and 3. In the analysis of these circRNA classifications, exonic circRNAs accounted for the largest proportion, up to 91.6%. This may be functionally related, as exonic circRNAs are derived directly from the exon region by back splicing, which protects them from "exon skipping" and makes them more likely to regulate the coding RNA that produces them [24-26].

We found that OVM significantly altered the circRNA expression profiles compared with normal orbital vessels. A total of 189 differentially expressed circRNAs were identified in OVM samples, of which 45 were upregulated and 144 were downregulated. We also identified 3,449 differentially expressed mRNAs and 324 differentially expressed miRNAs—that is, 2,175 upregulated mRNAs, 1,274 downregulated mRNAs, 156 upregulated miRNAs, and 168 downregulated miRNAs. qRT-PCR was performed to verify the circRNAs and mRNAs detected by RNA-seq. Five mRNAs (CALD1, RHOA, AES, CTSD, and LAPTM5) and three circRNAs (circRNA_2189, circRNA_3654, and circRNA_3192) were randomly selected, and the expression changes detected by qRT–PCR were in line with the RNA-seq results. CircRNAs mainly function as an important component of the ceRNA network, and circRNAs harboring miRNA response elements (MREs) that suppress miRNA activity by sponging miRNAs, thus upregulating the expression of target genes [27]. Subsequently, the circRNA–miRNA–mRNA ceRNA network was constructed using these differentially expressed mRNAs, circRNAs, and miRNAs.

Our comprehensive circRNA-associated network revealed the regulatory roles of circRNAs and their interactions with other RNAs in OVM. Further GO functional and KEGG pathway analyses were used to understand the potential functions of the mRNAs participating in the ceRNA network. GO functional analysis showed that the main related

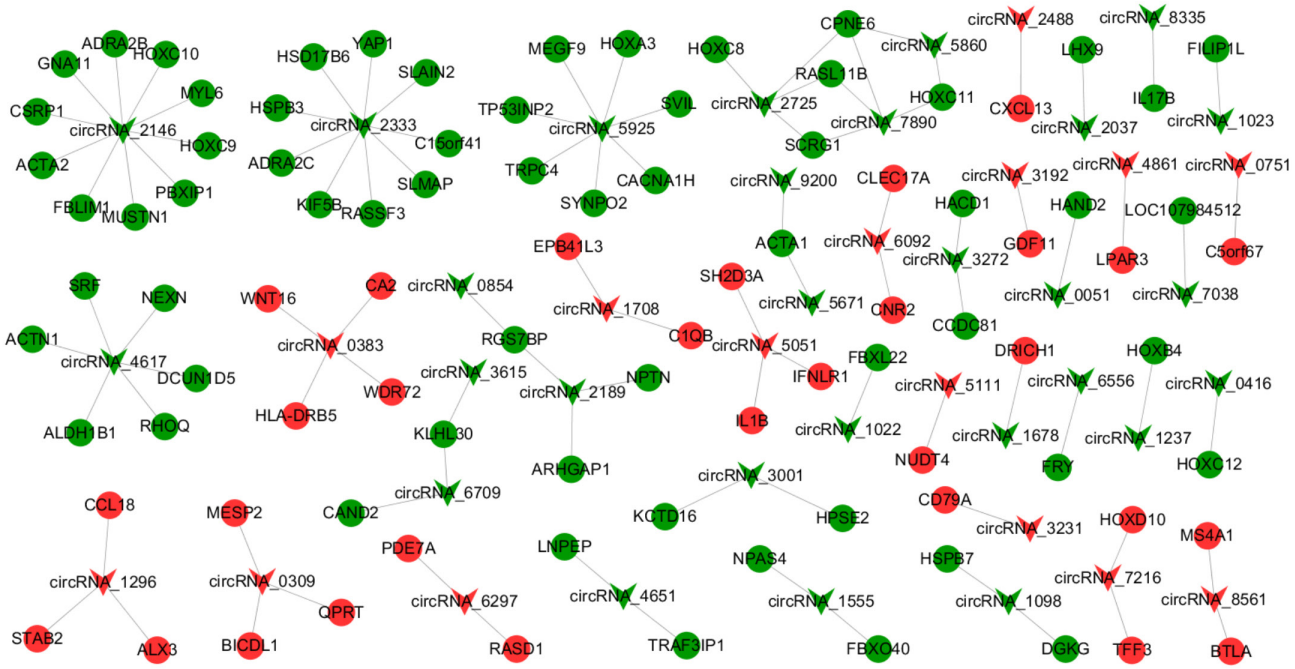

Figure 6. Coexpression network of differentially expressed mRNAs and circular RNAs (circRNAs). Dots represent mRNA and triangles represent circRNA. Red and green represent upregulated and downregulated RNAs, respectively.

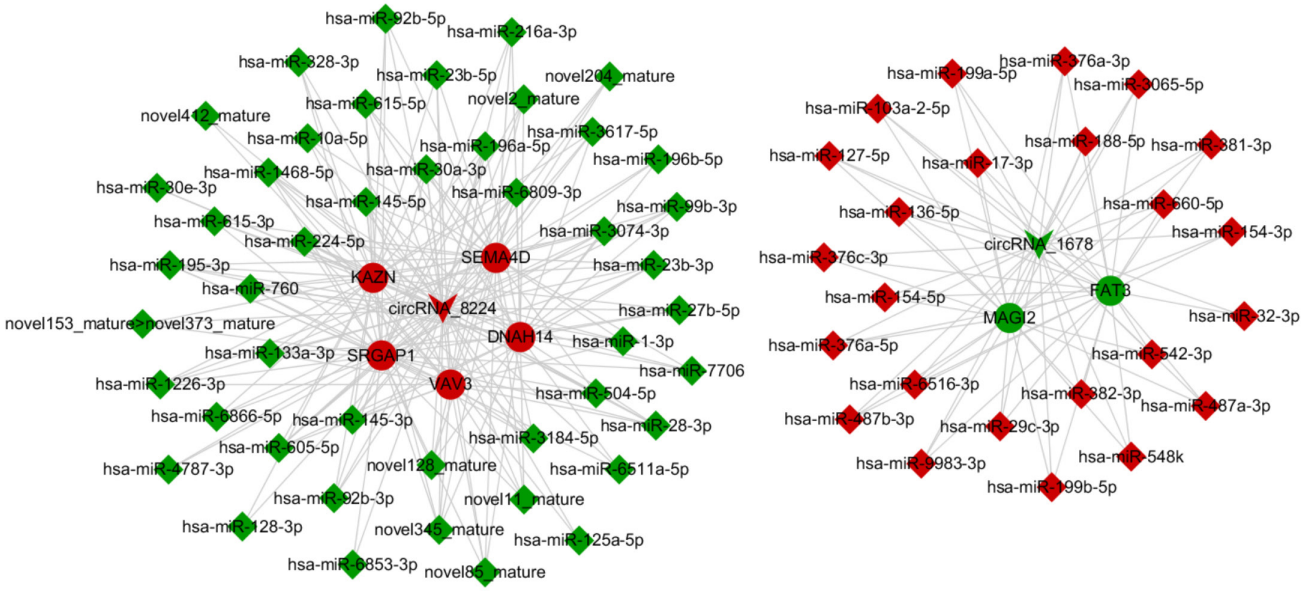

Figure 7. Circular RNA (circRNA)-associated competing endogenous RNA (ceRNA) networks in orbital venous malformation (OVM). CircRNA_8224 and CircRNA_1678 –associated ceRNA networks in OVM. Dots represent mRNA, triangles represent circiRNA, and squares represent miRNA. Red and green represent upregulated and downregulated RNAs, respectively.

BPs were enriched in extracellular matrix organization, positive regulation of actin nucleation, and so on. KEGG pathway analysis of upregulated mRNAs showed that mucin-type O-glycan biosynthesis, glycosaminoglycan degradation, and the PI3K-Akt signaling pathway were all enriched. In particular, the PI3K-Akt signaling pathway has been reported to be a critical regulator of vascular development and angiogenesis [28]. Previous studies have shown that somatic mutations of PIK3CA in the PI3K-Akt signaling pathway trigger the pathogenesis of capillary lymphatic venous malformation [29]. In addition, the PI3K-Akt signaling pathway has been reported to be involved in brain vascular malformations [30]. Here, we provide the first evidence that the PI3K-Akt signaling pathway is upregulated in OVMs, providing a potential mechanism of OVM formation.

In conclusion, our study is the first to unveil the profiles of circRNAs in OVM by RNA-seq analysis. Significantly differentially expressed circRNAs were identified in OVM tissues compared with normal orbital vessels, and a dysregulated circRNA-related ceRNA network was constructed to provide novel insight into the potential pathogenesis of OVM. Further exploration should focus on the precise molecular mechanisms of these circRNAs in OVM.

APPENDIX 1. CLINICAL INFORMATION OF OVM PATIENTS.

To access the data, click or select the words “Appendix 1.”

APPENDIX 2. CLINICAL INFORMATION OF UNAFFECTED PATIENTS.

To access the data, click or select the words “Appendix 2.”

APPENDIX 3. HISTOPATHOLOGICAL ANALYSIS OF OVM TISSUES AND NORMAL ORBITAL VASCULAR TISSUES.

To access the data, click or select the words “Appendix 3.” A and B. Hematoxylin and eosin (H.E.) staining of OVM tissues (A) and normal orbital vascular tissues (B). C and D. Immunohistochemical staining of CD34 in OVM tissues (C) and normal orbital vascular tissues (D).

APPENDIX 4. DIFFERENTIALLY EXPRESSED MRNAS IN OVM.

To access the data, click or select the words “Appendix 4.”

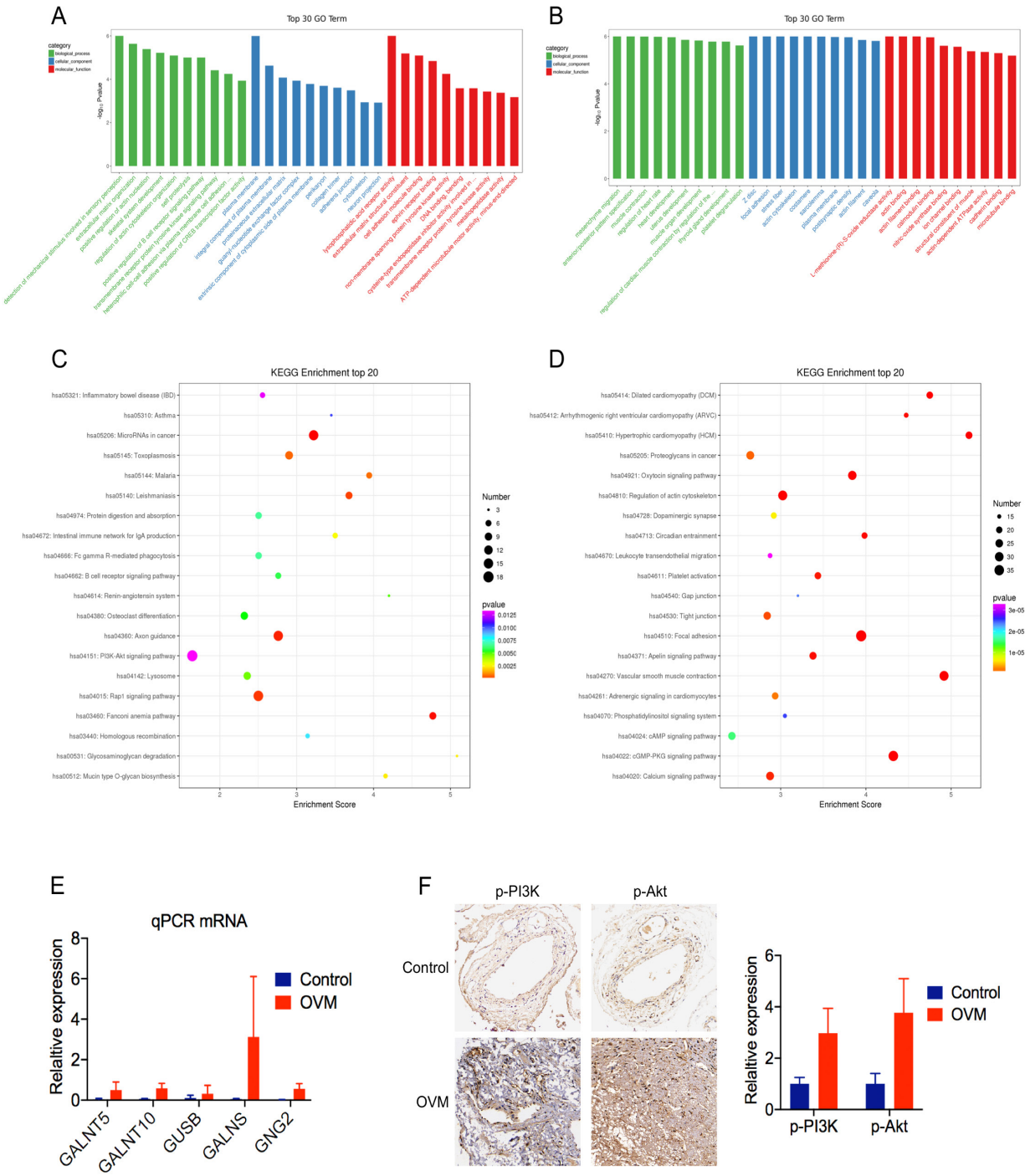

Figure 8. Gene Ontology (GO) and Kyoto Encyclopedia of Genes and Genomes (KEGG) analysis of the competing endogenous RNA (ceRNA) networks. **A**, **B**: The top 30 GO terms of biological process (BP), cellular component (CC), and molecular function (MF) categories for upregulated mRNAs (**A**) and downregulated mRNAs (**B**). **C**, **D**: The top 20 KEGG pathways of upregulated mRNAs (**C**) and downregulated mRNAs (**D**). **E**: The expression levels of representative genes in mucin-type O-glycan biosynthesis, glycosaminoglycan degradation and PI3K-Akt signaling pathway (GALNT5, GALNT10, GUSB, GALNS, GNG2) verified by quantitative real-time PCR (qRT-PCR). **F**: Representative images of immunohistochemical staining to p-PI3K and p-Akt in orbital venous malformation (OVM) and normal control samples and quantitative analysis.

APPENDIX 5. DIFFERENTIALLY EXPRESSED CIRCRNAS IN OVM.

To access the data, click or select the words "Appendix 5."

APPENDIX 6. DIFFERENTIALLY EXPRESSED MIRNAS IN OVM.

To access the data, click or select the words "Appendix 6."

APPENDIX 7. GO ANALYSES OF UPREGULATED MRNAS IN THE CERNA NETWORK.

To access the data, click or select the words "Appendix 7."

APPENDIX 8. GO ANALYSES OF DOWNREGULATED MRNAS IN THE CERNA NETWORK.

To access the data, click or select the words "Appendix 8."

APPENDIX 9. KEGG ANALYSES OF UPREGULATED MRNAS IN THE CERNA NETWORK.

To access the data, click or select the words "Appendix 9."

APPENDIX 10. KEGG ANALYSES OF DOWNREGULATED MRNAS IN THE CERNA NETWORK.

To access the data, click or select the words "Appendix 10."

APPENDIX 11. HEAT MAP OF GENES EXPRESSION IN MUCIN TYPE O-GLYCAN BIOSYNTHESIS, GLYCOSAMINOGLYCAN DEGRADATION, AND PI3K-AKT SIGNALING PATHWAY.

To access the data, click or select the words "Appendix 11." A. Heat map of genes expression in Mucin type O-glycan biosynthesis signaling pathway. B. Heat map of genes expression in glycosaminoglycan degradation signaling pathway. C. Heat map of genes expression in PI3K-Akt signaling pathway.

ACKNOWLEDGMENTS

We thank all thank all participants enrolled in our study and wish them good health. Funding; The current study was supported by the Natural Science Foundation of China (81570884, 81770961, 82103240), The Science and Technology Commission of Shanghai (20DZ2270800, 19JC1410200), Innovative research team of high-level local universities in Shanghai, and China Postdoctoral foundation funded project (1639). Ethics approval for this study was obtained from Shanghai JiaoTong University and this research was performed in accordance with the World Medical Association Declaration of Helsinki. Written informed consent was obtained from all involved patients or their guardians at the follow-up visit. Consent to publish Written informed consent was obtained from all involved patients. For children younger than 18 years, a form letter containing the carrier screening agreement was signed by their parents. Availability of data and materials Raw data reported in this paper, including RNA-seq, miRNA-seq data, have been deposited in the Gene Expression Omnibus database under accession number GSE158798. Yixiong Zhou (zhouyixiong212@gmail.com), Renbing Jia (renbingjia@sjtu.edu.cn) and Yefei Wang (paper34@163.com) are co-corresponding authors for this paper.

REFERENCES

1. Bonavolontà P, Fossataro F, Attanasi F, Clemente L, Iuliano A, Bonavolontà G. Epidemiological Analysis of Venous Malformation of the Orbit. J Craniofac Surg 2020; 31:759-61. [PMID: 31842075].
2. Hejazi N, Classen R, Hassler W. Orbital and cerebral cavernomas: comparison of clinical, neuroimaging, and neuropathological features. Neurosurg Rev 1999; 22:28-33. [PMID: 10348204].
3. Harris GJ, Jakobiec FA. Cavernous hemangioma of the orbit. J Neurosurg 1979; 51:219-28. [PMID: 448430].
4. Tan ST, Bialostocki A, Brasch H, Fitzjohn T. Venous malformation of the orbit. J Oral Maxillofac Surg 2004; 62:1308-11. .
5. Chung CF, Lai JS. Enophthalmos caused by an orbital venous malformation. Hong Kong Med J 2009; 15:299-300. .
6. Li T, Jia R, Fan X. Classification and treatment of orbital venous malformations: an updated review. Frontiers of medicine 2019; 13:547-55. [PMID: 30097960].
7. Young SM, Kim KH, Kim YD, Lang SS, Park JW, Woo KI, Lee JI. Orbital apex venous cavernous malformation with optic neuropathy: treatment with multisession gamma knife radiosurgery. Br J Ophthalmol 2019; 103:1453-9. [PMID: 30612095].
8. Arat YO, Mawad ME, Boniuk M. Orbital venous malformations: current multidisciplinary treatment approach. Arch Ophthalmol 2004; 122:1151-8. .
9. Chai P, Yu J, Li Y, Shi Y, Fan X, Jia R. High-throughput transcriptional profiling combined with angiogenesis antibody array analysis in an orbital venous malformation cohort. Exp Eye Res 2020; 191:107916-[PMID: 31926133].
10. Li Y, Yang L, Yang J, Shi J, Chai P, Ge S, Wang Y, Fan X, Jia R. A novel variant in GPAA1, encoding a GPI transamidase complex protein, causes inherited vascular anomalies with

various phenotypes. Hum Genet 2020; 139:1499-1511. [PMID: 32533362].

11. Huang XM, Yang WC, Liu Y, Tang DR, Wu T, Sun FY. Mutations in MC4R facilitate the angiogenic activity in patients with orbital venous malformation. Exp Biol Med (Maywood) 2020; 245:956-63. [PMID: 32363922].

12. Memczak S, Jens M, Elefsinioti A, Torti F, Krueger J, Rybak A, Maier L, Mackowiak SD, Gregersen LH, Munschauer M, Loewer A, Ziebold U, Landthaler M, Kocks C, le Noble F, Rajewsky N. Circular RNAs are a large class of animal RNAs with regulatory potency. Nature 2013; 495:333-8. [PMID: 23446348].

13. Shang Q, Yang Z, Jia R, Ge S. The novel roles of circRNAs in human cancer. Mol Cancer 2019; 18:6-[PMID: 30626395].

14. Jiang Q, Liu C, Li CP, Xu SS, Yao MD, Ge HM, Sun YN, Li XM, Zhang SJ, Shan K, Liu BH, Yao J, Zhao C, Yan B. Circular RNA-ZNF532 regulates diabetes-induced retinal pericyte degeneration and vascular dysfunction. J Clin Invest 2020; 130:3833-47. [PMID: 32343678].

15. Wu L, Zhou R, Diao J, Chen X, Huang J, Xu K, Ling L, Xia W, Liang Y, Liu G, Sun X, Qin B, Zhao C. Differentially expressed circular RNAs in orbital adipose/connective tissue from patients with thyroid-associated ophthalmopathy. Exp Eye Res 2020; 196:108036-[PMID: 32376473].

16. Rapaport F, Khanin R, Liang Y, Pirun M, Krek A, Zumbo P, Mason CE, Socci ND, Betel D. Comprehensive evaluation of differential gene expression analysis methods for RNA-seq data. Genome Biol 2013; 14:R95-[PMID: 24020486].

17. Wang L, Cao C, Ma Q, Zeng Q, Wang H, Cheng Z, Zhu G, Qi J, Ma H, Nian H, Wang Y. RNA-seq analyses of multiple meristems of soybean: novel and alternative transcripts, evolutionary and functional implications. BMC Plant Biol 2014; 14:169-[PMID: 24939556].

18. Li Y, Shang Q, Li P, Yang Z, Yang J, Shi J, Ge S, Wang Y, Fan X, Jia R. BMP9 attenuates occurrence of venous malformation by maintaining endothelial quiescence and strengthening vessel walls via SMAD1/5/ID1/α-SMA pathway. J Mol Cell Cardiol 2020; 147:92-107. [PMID: 32730768].

19. Li Y, Shang Q, Li P, Yang Z, Yang J, Shi J, Ge S, Wang Y, Fan X, Jia R. BMP9 attenuates occurrence of venous malformation by maintaining endothelial quiescence and strengthening vessel walls via SMAD1/5/ID1/α-SMA pathway. J Mol Cell Cardiol 2020; 147:92-107. [PMID: 32730768].

20. Kristensen LS, Andersen MS, Stagsted LVW, Ebbesen KK, Hansen TB, Kjems J. The biogenesis, biology and characterization of circular RNAs. Nat Rev Genet 2019; 20:675-91. [PMID: 31395983].

21. Su M, Xiao Y, Ma J, Tang Y, Tian B, Zhang Y, Li X, Wu Z, Yang D, Zhou Y, Wang H, Liao Q, Wang W. Circular RNAs in Cancer: emerging functions in hallmarks, stemness, resistance and roles as potential biomarkers. Mol Cancer 2019; 18:90-[PMID: 30999909].

22. Singh M, George AK, Homme RP, Majumder A, Laha A, Sandhu HS, Tyagi SC. Expression Analysis of the Circular RNA Molecules in the Human Retinal Cells Treated with Homocysteine. Curr Eye Res 2019; 44:287-93. [PMID: 30369271].

23. Ouyang XL, Chen BY, Xie YF, Wu YD, Guo SJ, Dong XY, Wang GH. Whole transcriptome analysis on blue light-induced eye damage. Int J Ophthalmol 2020; 13:1210-22. [PMID: 32821674].

24. Jeck WR, Sharpless NE. Detecting and characterizing circular RNAs. Nat Biotechnol 2014; 32:453-61. [PMID: 24811520].

25. Ebbesen KK, Hansen TB, Kjems J. Insights into circular RNA biology. RNA Biol 2017; 14:1035-45. [PMID: 27982727].

26. Eger N, Schoppe L, Schuster S, Laufs U, Boeckel JN. Circular RNA Splicing. Adv Exp Med Biol 2018; 1087:41-52. [PMID: 30259356].

27. Salmena L, Poliseno L, Tay Y, Kats L, Pandolfi PP. A ceRNA hypothesis: the Rosetta Stone of a hidden RNA language? Cell 2011; 146:353-8. [PMID: 21802130].

28. Tee AR, Blenis J. mTOR, translational control and human disease. Semin Cell Dev Biol 2005; 16:29-37. [PMID: 15659337].

29. Le Cras TD, Goines J, Lakes N, Pastura P, Hammill AM, Adams DM, Boscolo E. Constitutively active PIK3CA mutations are expressed by lymphatic and vascular endothelial cells in capillary lymphatic venous malformation. Angiogenesis 2020; 23:425-42. [PMID: 32350708].

30. Li QF, Decker-Rockefeller B, Bajaj A, Pumiglia K. Activation of Ras in the Vascular Endothelium Induces Brain Vascular Malformations and Hemorrhagic Stroke. Cell Reports 2018; 24:2869-82. [PMID: 30208313].

Articles are provided courtesy of Emory University and the Zhongshan Ophthalmic Center, Sun Yat-sen University, P.R. China. The print version of this article was created on 20 May 2022. This reflects all typographical corrections and errata to the article through that date. Details of any changes may be found in the online version of the article.